This is the author's peer reviewed, accepted manuscript. However, the online version of record will be different from this version once it has been copyedited and typeset.

PLEASE CITE THIS ARTICLE AS DOI: 10.1063/5.0138149

To Age or Not to Age: Anatomy of a Supercooled Liquid's Response to a High Alternating Electric Field

Ranko Richert

School of Molecular Sciences, Arizona State University, Tempe, Arizona 85287, United States

Abstract: Physical aging and structural recovery are the processes with which the structure of a system approaches equilibrium after some perturbation. Various methods exist that initiate structural recovery, such as changing temperature or applying a strong external static field. This work is concerned with high alternating electric fields and their suitability to study structural recovery and aging. The present work demonstrates that rationalizing the nonlinear dielectric response of a supercooled liquid to high amplitude ac-fields requires multiple fictive temperatures. This feature is in stark contrast to structural recovery after a temperature down-jump or a considerable increase in the static electric field, for which a single parameter, fictive temperature or material time, describes the structural change. In other words, the structural recovery from a high ac-field does not adhere to time - aging time superposition, which is so characteristic of genuine aging processes.

Keywords: physical aging, structural recovery, fictive temperatures, nonlinear dielectric responses.

Corresponding author e-mail: ranko@asu.edu

PLEASE CITE THIS ARTICLE AS DOI: 10.1063/5.0138149

I. INTRODUCTION

The relation that connects physical aging with the primary or α -relaxation (often referred to as 'structural relaxation') is subject to continued interest. 1,2,3 The α -relaxation dynamics or its time constant τ_{α} are usually derived from relaxation experiments in the regime of linear response,⁴ and thus equivalent to the dynamics of equilibrium fluctuations.⁵ The classical approach to physical aging is based on a temperature down-jump from an equilibrium state to a temperature at which the process of reaching equilibrium is slow compared with the time it takes to realize the temperature change. Therefore, the aging temperature, T_{age} , would be below or far below the glass transition temperature $T_{\rm g}$, often hampering a measurement of $au_{
m a}$ at $T_{
m age}$ for a direct comparison with the aging dynamics. The progress of physical aging can be monitored via a change in volume, ⁶ enthalpy, or susceptibility at a given frequency. For large excursions from equilibrium, the subsequent aging will be affected by changes of the relaxation time scale as the system adapts its structure towards that of the equilibrium state. ^{9,10} This process is typically accounted for by models such as the Tool-Narayanaswamy-Moynihan (TNM)¹¹ or Kovacs-Aklonis-Hutchinson-Ramos $(KAHR)^{12}$ formalisms in terms of the concept of fictive temperature, $T_{\rm fic}$, or material time, ξ . As an approximation, the value of T_{fic} characterizes the structure of a nonequilibrium state via the temperature that would lead to the same structure if the system was in equilibrium. 14,15

In order to facilitate an unambiguous comparison between equilibrium fluctuations in terms of τ_{α} and the dynamics of physical aging, two objectives may be pursued: (i) Moving $T_{\rm age}$ to above $T_{\rm g}$ so that τ_{α} at $T_{\rm age}$ can be determined directly; and (ii) using very small perturbations to initiate aging so that changes of τ_{α} in the course of the aging process remain negligible. We will refer to such aging processes in the limit of small perturbations as structural recovery, a situation for which models such as TNM or KAHR need not be invoked. In fact, these models predict that structural recovery will follow the dynamics characterized by τ_{α} or 'structural relaxation', a feature that has not been verified experimentally.¹⁶

The realization of physical aging or structural recovery at $T > T_g$ and thus at readily accessible values of τ_{α} was possible via one of two options: Cryostats that allow for very fast temperature jumps,¹⁷ or perturbing the system with electric fields of sufficiently high magnitude.^{16,18,19} It has been demonstrated that a large amplitude static (dc) field results in a shift towards increased relaxation times,^{20,21,22} qualitatively analogous to a temperature down-jump. These high dc-field

PLEASE CITE THIS ARTICLE AS DOI: 10.1063/5.0138149

experiments have shown that the aging response is up to a factor of about 3 slower than τ_{α} , with the factor τ_{age}/τ_{α} being material specific. These factors are consistent with $\tau_{age} \approx \tau_{ex}$, with τ_{ex} being the time scale of rate exchange, i.e., the rate of time constant fluctuations in equilibrium. 1,23,24 In the present study, we investigate whether the application of a high alternating electric field without dc bias is a suitable alternative to initiate structural recovery or physical aging. Based on results for propylene carbonate, 25 it is found that the response of a supercooled liquid to a substantial amplitude jump of the ac electric field does not resemble the physical aging behavior resulting from temperature or dc-field changes. In particular, the feature of time - aging time superposition (TaTS), which is highly characteristic of physical aging, is not reproduced with large alternating fields.

II. MODEL CONSIDERATIONS

The model outlined below has been employed successfully for describing the nonlinear dielectric response of supercooled liquids to a large amplitude ac electric field with no dc-bias, $E(t) = E_0 \sin(\omega_0 t)$, with step-like changes of the peak amplitude E_0 . This includes the more complex field protocols employed in dielectric hole burning experiments, $e^{27,28,29,30}$ aimed at demonstrating the heterogeneous nature of structural relaxation. Accordingly, the model assumes heterogeneous dynamics, i.e., a set of $e^{23,24,31}$ Accordingly, the model constants $e^{23,24,31}$ and $e^{23,24,31}$ with time constants $e^{23,24,31}$, such that the linear response permittivity, $e^{23,24,31}$ are $e^{23,24,31}$ and $e^{23,24,31}$ are $e^{23,24,31}$ and $e^{23,24,31}$ are $e^{23,24,31}$ and $e^{23,24,31}$ are $e^{23,24,31}$ and $e^{23,24,31}$ are $e^{23,24,31}$ are $e^{23,24,31}$ and $e^{23,24,31}$ are $e^{23,24,31}$ and $e^{23,24,31}$ are $e^{23,24,31}$ and $e^{23,24,31}$ are $e^{23,24,31}$ are $e^{23,24,31}$ and $e^{23,24,31}$ are $e^{23,24,31}$ and $e^{23,24,31}$ are $e^{23,24,31}$ and $e^{23,24,31}$ are $e^{23,24,31}$ and $e^{23,24,31}$ are $e^{23,24,31}$ are $e^{23,24,31}$ and $e^{23,24,31}$ are $e^{23,24,31}$ and $e^{23,24,31}$ are $e^{23,24,31}$ are $e^{23,24,31}$ are $e^{23,24,31}$ and $e^{23,24,31}$ are $e^{23,24,31}$ and $e^{23,24,31}$ are $e^{23,24,31}$ are $e^{23,24,31}$ and $e^{23,24,31}$ are $e^{23,24,31}$ and $e^{23,24,31}$ are $e^{23,24,31}$ are $e^{23,24,31}$ and $e^{23,24,31}$ are $e^{23,24,31}$ and $e^{23,24,31}$ are $e^{23,24,31}$ and $e^{23,24,31}$ are $e^{23,24,31}$ and $e^{23,24,31}$ are $e^{23,24,31}$ are $e^{23,24,31}$ and $e^{23,24,31}$ are $e^{23,24,31}$ are $e^{23,24,31}$ and $e^{23,24,31}$ ar

$$\varepsilon^*(\omega) = \varepsilon_{\infty} + \sum_{i=1}^{N} \frac{\Delta \varepsilon_i}{1 + i\omega \tau_i},\tag{1}$$

with the amplitudes $\Delta \varepsilon_i$ chosen to match the experimental loss profile. The main effect of the high field is to increase the fictive temperatures T_i of the individual modes, thereby leading to reduced values of the τ_i 's. The dielectric properties are obtained from the field E(t) and the resulting modespecific displacement $D_i(t)$,

$$\frac{dD_i(t)}{dt} = \frac{\varepsilon_0 E(t) \Delta \varepsilon_i}{\tau_i(t)} - \frac{D_i(t)}{\tau_i(t)},\tag{2}$$

with initial conditions $E(t \le 0) = 0$, $D_i(t \le 0) = 0$, and $T_i(t \le 0) = T$. To match the experimental conditions of a 10 μ m sample thickness combined with the electrodes acting as heat reservoirs, the real temperature T is held constant.

PLEASE CITE THIS ARTICLE AS DOI: 10.1063/5.0138149

For each mode, the rate of energy absorption from the field is given by the power density p_i via

$$p_i = \varepsilon_0 E_0^2 \varepsilon_i^{"}(\omega) \omega / 2 = j_i^2(t) \tau_i(t) / (\varepsilon_0 \Delta \varepsilon_i), \qquad (3)$$

where $j_i = dD_i/dt$ is the current density and ε_0 is the permittivity of vacuum. The modification of the fictive temperature is given by a gain term, $p_i/\rho\Delta C_{p,i}$ and a loss term $(T_i(t) - T)/\tau_i(t)$ that mimics heat flow to the phonon reservoir, where $\rho\Delta C_{p,i}$ is the volumetric heat capacity of mode 'i'. The values of T_i are thus determined by

$$\frac{dT_i(t)}{dt} = \frac{j_i^2(t)\tau_i(t)}{\varepsilon_0 \Delta \varepsilon_i \rho \Delta C_{ni}} - \frac{T_i(t) - T}{\tau_i(t)},\tag{4}$$

and the time constants adjust to T_i according to $d \ln \tau_i = E_A d(1/k_B T_i)$. Solving the above differential equations for sufficiently small time steps while obtaining the total current density from $j(t) = j_{\infty}(t) + \sum_i j_i(t)$ facilitates the determination of $\tan \delta = \varepsilon''/\varepsilon'$ from the phase angles ϕ of the field and current density as $\tan(\pi/2 - \phi_E + \phi_j)$ for each period of duration $2\pi/\omega$. It should be noted that this calculation recovers the experimental loss profile $\varepsilon''(\omega)$ with high fidelity, provided E_0 is kept sufficiently small.

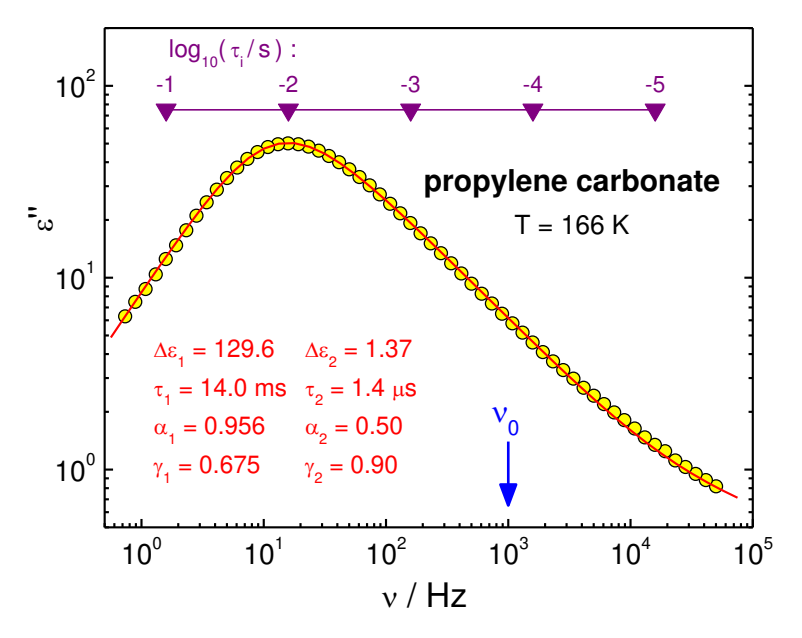


Fig. 1. Symbols represent the dielectric loss profile, $\varepsilon''(\omega)$, of propylene carbonate measured at T=166 K, taken from Ref. 25. The line is a fit according to Eq. (5) with the parameters given in the legend. The arrow indicates the frequency v_0 at which the high-field experiments are performed. The triangles identify the positions of integer values of $\log_{10}(\tau_i/s)$, with $\tau=1/(2\pi v)$.

PLEASE CITE THIS ARTICLE AS DOI: 10.1063/5.0138149

III. RESULTS AND DISCUSSION

The present analysis of high ac-field effects relies on a previous measurement involving propylene carbonate (PC) at T = 166 K. The dielectric loss profile of PC at T = 166 K is shown in Fig. 1, together with a double Havriliak-Negami (HN) fit using

$$\varepsilon^*(\omega) = \varepsilon_{\infty} + \frac{\Delta \varepsilon_1}{[1 + (i\omega\tau_1)^{\alpha_1}]^{\gamma_1}} + \frac{\Delta \varepsilon_2}{[1 + (i\omega\tau_2)^{\alpha_2}]^{\gamma_2}},\tag{5}$$

with the parameters given in the legend of Fig. 1. The second and smaller HN peak is added to account for the secondary relaxation that leads to deviation from the high frequency power law for v > 2 kHz.

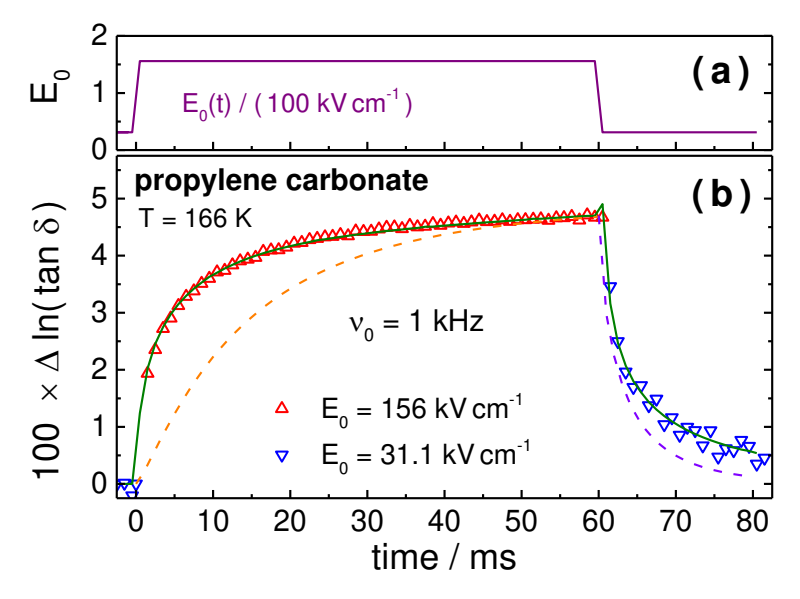


Fig. 2. (a) Time dependent variation of the peak field amplitude E_0 of the sinusoidal field with frequency $v_0 = 1$ kHz. (b)Time resolved non-linear dielectric effect for propylene carbonate at T = 166 K, shown in terms of the relative change of the loss tangent, $\Delta \ln(\tan \delta)$, with time. Experimental results are displayed as symbols for the 60 periods following the transition from low ($E_0 = 31.1$ kV cm⁻¹) to high ($E_0 = 156$ kV cm⁻¹) field at t = 0 and the 20 periods following the transition to the low field at t = 60 ms. The solid line represents the model calculation following Eq. (1) through Eq. (4) as described in the text. The dashed lines indicate the behavior expected if aging followed the relaxation dynamics, determined via Eq. (6).

The result of switching from a low to a high field amplitude is depicted in Fig. 2b. It shows a gradual rise of $\tan \delta$ at $v_0 = 1$ kHz due to the peak field amplitude being increased by a factor of 5 at t = 0, followed by a return toward the low field value after the field is reduced again at t = 60 ms, see Fig. 2a for the field amplitude pattern. Note that the changes observed for the experimentally more robust quantity $\tan \delta$ are dominated by those of ε'' , while ε' is practically constant. The important feature of this graph is the model calculation along Eq. (1) through Eq.

PLEASE CITE THIS ARTICLE AS DOI: 10.1063/5.0138149

(4) represented as solid line, and how well it matches the experimental finding with practically no adjustable parameter. For details see the original discussion of this experiment and modeling.²⁵

The Fig. 2 also includes as dashed lines the structural recovery that would be expected if it followed the dielectric relaxation dynamics in the limit of linear response. To determine these curves, the prominent loss peak of Eq. (5) has been translated into the equivalent time domain representation, i.e., a stretched exponential of the form $\varepsilon(t) = \varepsilon_{\infty} + \Delta \varepsilon \times \exp\left[-(t/\tau_{KWW})^{\beta}\right]$. The relations used, 32 $\beta_{KWW} = (\alpha_{HN}\gamma_{HN})^{0.83}$ and $log(\tau_{KWW}) = log(\tau_{HN}) - 2.5 \exp(-3.5\beta_{KWW})$, have been derived from fitting HN spectra with the Fourier transform of KWW decays 33 and by moment analysis of the HN and KWW distributions, 34 and lead to the parameters $\tau_{KWW} = 8.43$ ms and $\beta = 0.69$. Because the nonlinear dielectric effect of Fig. 2 is quadratic in E_0 , the field induced structural recovery based upon a stretched exponential is expected to follow

$$\tan\delta \propto \left(1 - exp\left[-(t/\tau_{KWW})^{\beta}\right]\right)^{2}$$
, and (6a)

$$\tan\delta \propto \left(exp\left[-(t/\tau_{KWW})^{\beta}\right]\right)^{2}$$
, (6b)

for the rise and decay, respectively.²² Already from this graph it becomes obvious that adjusting τ_{KWW} in Eq. (6) will not make the dashed curves in Fig. 2b coincide with the experimental structural recovery result, because the rise is too slow and the decay too fast. By contrast, analogous experiments based on high dc-fields reveal that equilibrium relaxation and structural recovery dynamics are very similar, and for some materials practically identical.^{14,22}

Because the model outlined above reproduces the time dependent shift of relaxation time constants and the concomitant change of $\tan \delta$ at a fixed frequency so well, it can be used to reveal the origin of the marked difference between structural recovery initiated by a large ac field and the equilibrium relaxation dynamics at the same temperature. Fig. 3 shows the time dependent fictive temperatures for various relaxation modes with $\log_{10}(\pi/s)$ between -1 and -5, with this range of π being identified relative to the loss profile in Fig. 1. These $T_i(t, \pi_i)$ curves approach limiting values given by

$$T_i(t \to \infty) = T + \frac{\varepsilon_0 E_0^2 \Delta \varepsilon}{2\rho \Delta C_p} \times \frac{\omega_0^2 \tau_i^2}{1 + \omega_0^2 \tau_i^2},\tag{7}$$

with $\omega_0 = 2\pi \nu_0$. This relation emerges directly from Eq. (3) and Eq. (4) in the steady state limit, and the magnitude of T_i is a matter of the balance of the rates of energy influx by absorption from

PLEASE CITE THIS ARTICLE AS DOI: 10.1063/5.0138149

the field and energy loss to the phonon bath, resulting in a strong dependence on the value of π . Clearly, each mode approaches its final fictive temperature, $T_i(t \to \infty)$, on a time scale given by τ_i itself, which is the hallmark of heterogeneous dynamics.

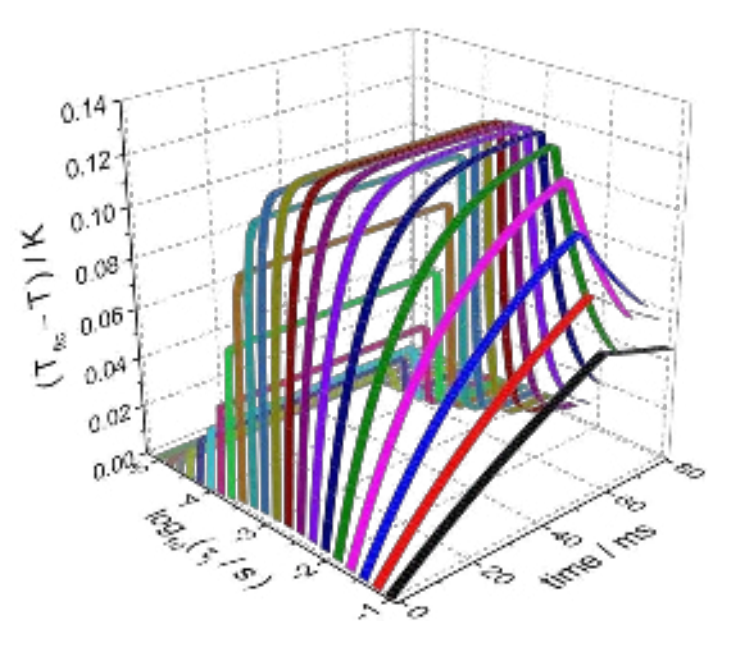


Fig. 3. Model calculation of the mode specific fictive temperatures, $T_i(t,\tau_i)$, as a function of time t and time constant τ_i . The calculation is based on the same parameters that lead to the solid line in Fig. 2. The integer values of $\log_{10}(\pi/s)$ between -5 and -1 are indicated as triangles in Fig. 1 in order to clarify the present range of $\log_{10}(\tau_i/s)$ relative to the loss profile $\varepsilon''(\nu)$.

What remains obscured in Fig. 3 is the extent to which a $T_i(t)$ curve for a given τ_i affects the dielectric loss ε'' or equivalently $\tan \delta$ at the measurement frequency ν_0 , 1 kHz in the present case. In order to judge how the $T_i(t)$ curve of mode 'i' affects the value of $\varepsilon''(\nu_0)$, Fig. 4 depicts the product of $(T_{\text{fic}} - T)$ and the loss $\varepsilon_i''(\nu_0)$ of mode 'i' at the frequency ν_0 . Note that the dielectric loss of mode 'i' is a Debye type profile given by $\varepsilon_i''(\omega) = \Delta \varepsilon_i \, \omega^2 \tau_i^2 / (1 + \omega^2 \tau_i^2)$. The curves in Fig. 4 are similar to those of Fig. 3, but now weighted by how much influence a $T_i(t)$ curve has on the experimentally relevant quantity $\varepsilon''(\nu_0)$ or $\tan \delta(\nu_0)$. This leads to a bimodal profile of the effective change at v_0 as a function of $\log_{10}(\tau_0/s)$. These results reveal that the field induced modification of $\varepsilon''(\nu_0)$ is dominated by two time constant bands, one near $\log_{10}(\tau/s) = -3.4$ and one near $\log_{10}(\tau/s)$ = -2.0, with the former resulting from the position of test frequency $v_0 = 1$ kHz and the latter from that of $v_{\text{max}} = 16 \text{ Hz}$, the peak frequency of the low field dielectric loss profile. This bimodal feature explains why the relative change of $\tan \delta$ in Fig. 2 displays a very fast component (practically

PLEASE CITE THIS ARTICLE AS DOI: 10.1063/5.0138149

- Fublishing Chemical Physic

instantaneous at the time resolution of one period with duration $1/\nu_0$), followed by a slow approach to equilibrium whose time scale is relatively close to that of the α -relaxation.

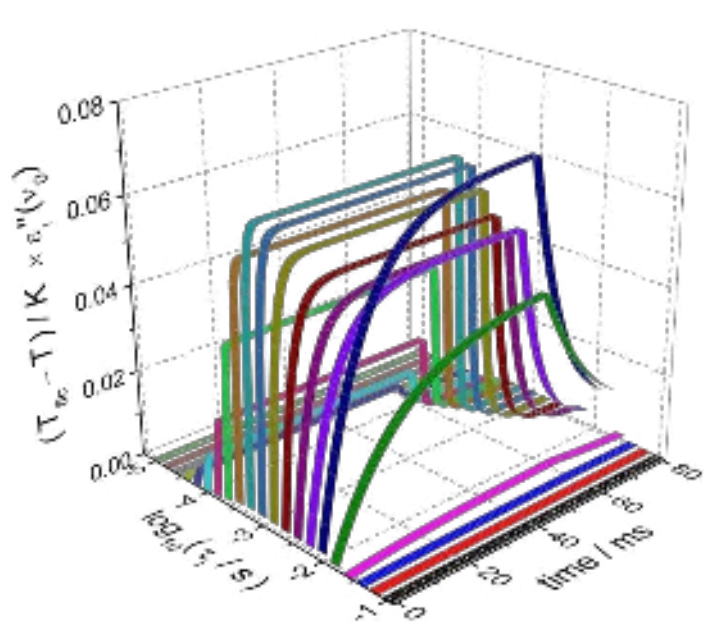


Fig. 4. Model calculation of the mode specific fictive temperatures, $T_i(t, \tau_i)$, multiplied by the loss of mode 'i' at the test frequency $v_0 = 1$ kHz, $\varepsilon_i''(v_0)$. The calculation is based on the same parameters that lead to the solid line in Fig. 2. The integer values of $\log_{10}(\tau_i/s)$ between -5 and -1 are indicated as triangles in Fig. 1 in order to clarify the present range of $\log_{10}(\tau_i/s)$ relative to the loss profile $\varepsilon''(v)$.

As mentioned already, the model employed here is based on heterogeneous dynamics, implying that different modes can be associated with different fictive temperatures, as obvious in Fig. 3. By contrast, it is well established by experimental evidence that structural recovery and physical aging can be rationalized via a single fictive temperature. ^{8,13,16} This situation is illustrated in Fig. 5, where fast and slow modes all follow a common pattern with respect to time. It is exactly this scenario of homogeneous structural recovery that leads to the feature of TaTS, equivalent to the loss profile shifting as a whole, ³⁵ instead of fast modes approaching equilibrium faster than slow ones. ^{8,16,36}

Recently, Moch *et al.* have performed a high ac-field experiment analogous to the one discussed in this study, but on propylene glycol (PG) at T = 163.8 K using a frequency of $\nu_0 = 0.1$ Hz.³⁷ Their $\varepsilon''(t)$ result is shown in Fig. 6 and follows the pattern predicted by the present model, even quantitatively if it is recognized that the time scale of the nonlinear response stops accelerating with increasing distance between ν_0 and ν_{max} .^{18,25} Unlike the case of Fig. 3, the

PLEASE CITE THIS ARTICLE AS DOI: 10.1063/5.0138149

situation of $v_0 >> v_{\text{max}}$ associated with the data of Fig. 6 leads to the expectation that the present model will match only after adjusting the time scale. Such a calculation based on the model of Eq. (1) to Eq. (4) is included as solid line in Fig. 6, and agrees well with the data for PG (the spikes at times t = 0 and 12,200 s are real and originate from the polarization adjusting only slowly to the abrupt change in field amplitude). In the work by Moch et al., 37 the PG data have been analyzed by fitting the slow components of the rise and decay, i.e., without the 'instantaneous' contribution that originates from modes with $\tau \approx 1/(2\pi \nu_0)$. According to Fig. 4, such an analysis focuses on the $T_{\rm fic}(t)$ band around $\tau_{\rm i} = \tau_{\rm max}$, and is thus expected by the present model to yield a time dependence similar to that of the primary dielectric relaxation, as has been found for PG.³⁷ Nevertheless, such a measurement does not represent structural recovery as observed by a temperature decrease or a dc-field increase, because the nonlinear ac-field experiment involves more than a single fictive temperature.

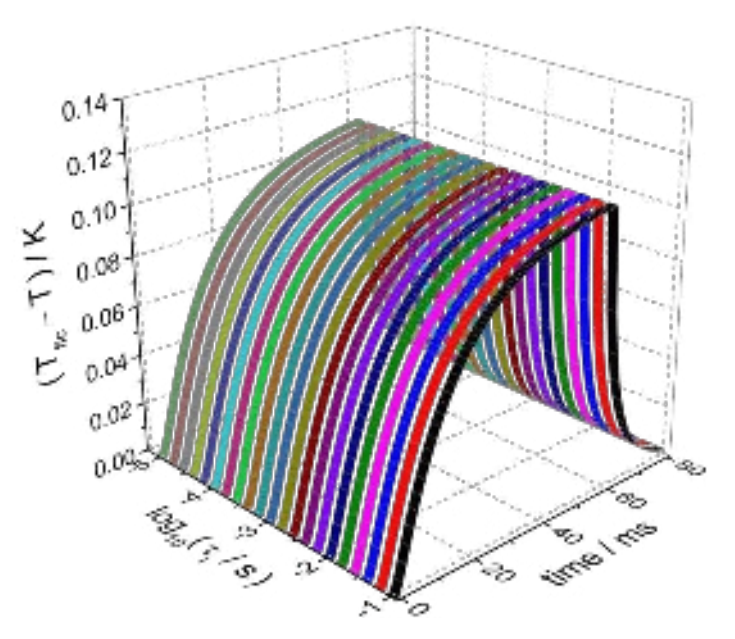


Fig. 5. Calculation of mode specific fictive temperatures, $T_i(t, \tau_i)$, assuming that all modes follow the α -relaxation dynamics according to Eq. (6) and independent of τ_i . The calculation is based on the same parameters that lead to the dashed lines in Fig. 2. The integer values of $\log_{10}(\pi/s)$ between -5 and -1 are indicated as triangles in Fig. 1 in order to clarify the present range of $\log_{10}(\tau_i/s)$ relative to the loss profile $\varepsilon''(\nu)$.

From the present study, it has to be concluded that the process of a liquid approaching equilibrium with a large amplitude ac-field is very different from physical aging and structural recovery as we know it. The interesting question is: why can distinct modes modify their time

Chemical Physics

This is the author's peer reviewed, accepted manuscript. However, the online version of record will be different from this version once it has been copyedited and typeset

PLEASE CITE THIS ARTICLE AS DOI: 10.1063/5.0138149

constants π independently when absorbing energy from an external field, while they follow a common fictive temperature when subject to a decrease of the temperature or an increase of the static electric field? Two possible explanations come to mind: (i) shifting modes toward higher frequencies (as with structural recovery from an ac-field) differs qualitatively from the classical case of shifting modes toward lower frequencies (as with dc-fields and temperature down-jumps); (ii) another feature that distinguishes the ac-field effect from others is that only a subset of modes are involved in the nonlinear response, as specified by the power spectrum of the high field. At this point, a solution to this conundrum does not appear to exist.

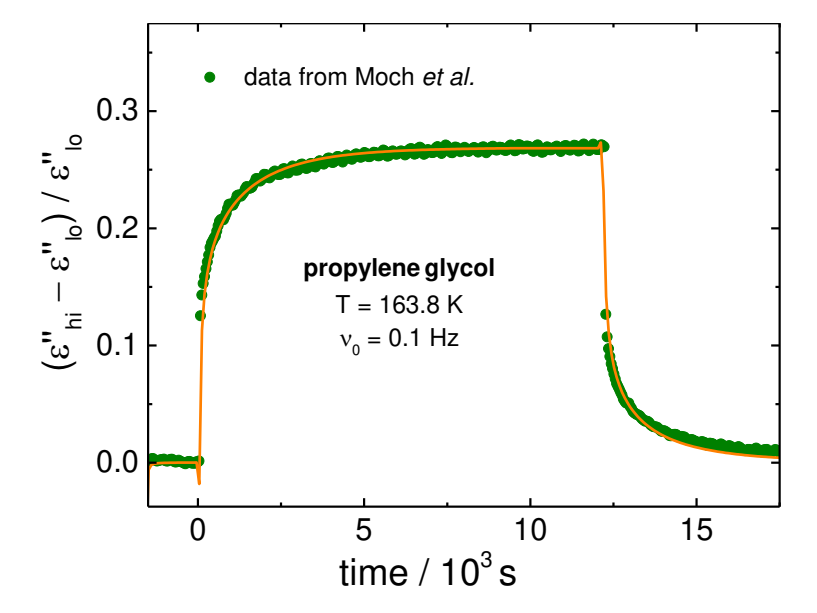


Fig. 6. Time resolved non-linear dielectric effect for propylene glycol at T = 163.8 K, reported by Moch *et al.*, Ref. 37. The results are shown as symbols in terms of the relative change of the dielectric loss versus time. The high amplitude ac field has been applied for times $0 \le t \le 12,200$ s. The solid line represents the model calculation following Eq. (1) through Eq. (4) as described in the text, using $\alpha_{\text{HN}} = 0.98$, $\gamma_{\text{HN}} = 0.70$, and $\tau_{\text{HN}} = 300$ s.

IV. SUMMARY AND CONCLUSIONS

This work employed existing nonlinear dielectric results based on high amplitude sinusoidal fields with no dc-bias to answer whether the field induced shifts of time constants resemble the typical features of physical aging and structural recovery. The time resolved changes of $\varepsilon''(\nu_0)$ resulting from an ac-field amplitude increase can be explained entirely by increases in fictive temperatures and the concomitant reduction of time constant values, as demonstrated by the model that quantifies the effects of energy absorption from the electric field. However, this nonlinear effect is shown to be incompatible with the time - aging time superposition that is so characteristic

This is the author's peer reviewed, accepted manuscript. However, the online version of record will be different from this version once it has been copyedited and typeset. PLEASE CITE THIS ARTICLE AS DOI: 10.1063/5.0138149

of structural recovery and aging processes. In other words, the response to a high ac-field cannot be rationalized by a single fictive temperature, but rather requires a set of mode specific fictive temperatures. As a consequence, high ac-fields are not recommended for studying structural recovery and physical aging.

ACKNOWLEDGMENTS

This research was supported by the National Science Foundation under grant numbers DMR-1904601.

AUTHOR DECLARATIONS

Conflict of Interest

The author has no conflicts of interest to disclose.

DATA AVAILABILITY

The data that support the findings of this study are available from the corresponding author upon reasonable request.

REFERENCES

- R. Richert, J. P. Gabriel, and E. Thoms, "Structural relaxation and recovery: A dielectric approach," J. Phys. Chem. Lett. 12, 8465 (2021).
- K. Moch, P. Münzner, R. Böhmer, and C. Gainaru, "Molecular cross-correlations govern structural rearrangements in a nonassociating polar glass former," Phys. Rev. Lett. 128, 228001 (2022).
- S. Mehri, L. Costigliola, and J. C. Dyre, "Single-parameter aging in the weakly nonlinear limit," Thermo 2, 160 (2022).
- C. A. Angell, K. L. Ngai, G. B. McKenna, P. F. McMillan, and S. W. Martin, "Relaxation in glassforming liquids and amorphous solids," J. Appl. Phys. 88, 3113 (2005).
- R. Kubo, "The fluctuation-dissipation theorem," Rep. Prog. Phys. 29, 255 (1966).
- A. J. Kovacs, "La contraction isotherme du volume des polymères amorphes," J. Polym. (6) Sci. 30, 131 (1958).
- I. M. Hodge, "Enthalpy relaxation and recovery in amorphous materials," J. Non-Cryst. Solids **169**, 211 (1994).
- P. Lunkenheimer, R. Wehn, U. Schneider, and A. Loidl, "Glassy aging dynamics," Phys. Rev. Lett. 95, 055702 (2005).

- . However, the online version of record will be different from this version once it has been copyedited and typeset. PLEASE CITE THIS ARTICLE AS DOI: 10.1063/5.0138149 This is the author's peer reviewed, accepted manuscript. However,

- A. Q. Tool, "Relation between inelastic deformability and thermal expansion of glass in its annealing range," J. Am. Ceram. Soc. **29**, 240 (1946).
- (10) O. S. Narayanaswamy, "A model of structural relaxation in glass," J. Am. Ceram. Soc. 54, 491 (1971).
- (11) M. A. DeBolt, A. J. Easteal, P. B. Macedo, and C. T. Moynihan, "Analysis of structural relaxation in glass using rate heating data," J. Am. Ceram. Soc. **59**, 16 (1976).
- (12) A. J. Kovacs, J. J. Aklonis, J. M. Hutchinson, and A. R. Ramos, "Isobaric volume and enthalpy recovery of glasses. II. A transparent multiparameter theory," J. Polym. Sci. Polym. Phys. Ed. 17, 1097 (1979).
- (13) B. Riechers, L. A. Roed, S. Mehri, T. S. Ingebrigtsen, T. Hecksher, J. C. Dyre, and K. Niss, "Predicting nonlinear physical aging of glasses from equilibrium relaxation via the material time," Sci. Adv. 8, eabl9809 (2022).
- (14) B. Riechers and R. Richert, "Structural recovery and fictive variables: The fictive electric field," Thermochim. Acta 677, 54 (2019).
- (15) K. Niss, "A density scaling conjecture for aging glasses," J. Chem. Phys. **157**, 054503 (2022).
- (16) B. Riechers and R. Richert, "Rate exchange rather than relaxation controls structural recovery," Phys. Chem. Chem. Phys. 21, 32 (2019).
- (17) T. Hecksher, N. B. Olsen, K. Niss, and J. C. Dyre, "Physical aging of molecular glasses studied by a device allowing for rapid thermal equilibration," J. Chem. Phys. 133, 174514 (2010).
- (18) S. Samanta and R. Richert, "Limitations of heterogeneous models of liquid dynamics: Very slow rate exchange in the excess wing," J. Chem. Phys. 140, 054503 (2014).
- (19) R. Richert, "One experiment makes a direct comparison of structural recovery with equilibrium relaxation," J. Chem. Phys. **157**, 224501 (2022).
- (20) G. P. Johari, "Effects of electric field on the entropy, viscosity, relaxation time, and glassformation," J. Chem. Phys. 138, 154503 (2013).
- (21) S. Samanta and R. Richert, "Dynamics of glass-forming liquids. XVIII. Does entropy control structural relaxation times?," J. Chem. Phys. 142, 044504 (2015).
- (22) A. R. Young-Gonzales, S. Samanta, and R. Richert, "Dynamics of glass-forming liquids. XIX. Rise and decay of field induced anisotropy in the non-linear regime," J. Chem. Phys. **143**, 104504 (2015).
- (23) M. D. Ediger, "Spatially heterogeneous dynamics in supercooled liquids," Annu. Rev. Phys. Chem. **51**, 99 (2000).

PLEASE CITE THIS ARTICLE AS DOI: 10.1063/5.0138149

- (24) R. Richert, "Heterogeneous dynamics in liquids: Fluctuations in space and time," J. Phys.: Condens. Matter 14, R703 (2002).
 (25) W. Huang and R. Richert, "Dynamics of glass-forming liquids. XIII. Microwave heating in slow motion," J. Chem. Phys. 130, 194509 (2009).
- (26) R. Richert, "Reverse calorimetry of a supercooled liquid: Propylene carbonate," Thermochim. Acta **522**, 28 (2011).
- (27) B. Schiener, R. Böhmer, A. Loidl, and R. V. Chamberlin, "Nonresonant spectral hole burning in the slow dielectric response of supercooled liquids," Science **274**, 752 (1996).
- (28) B. Schiener, R. V. Chamberlin, G. Diezemann, and R. Böhmer, "Nonresonant dielectric hole burning spectroscopy of supercooled liquids," J. Chem. Phys. **107**, 7746 (1997).
- (29) K. R. Jeffrey, R. Richert, and K. Duvvuri, "Dielectric hole burning: signature of dielectric and thermal relaxation time heterogeneity," J. Chem. Phys. **119**, 6150 (2003).
- (30) T. Blochowicz and E. A. Rössler, "Nonresonant dielectric hole burning in neat and binary organic glass formers," J. Chem. Phys. **122**, 224511 (2005).
- (31) R. Böhmer, R. V. Chamberlin, G. Diezemann, B. Geil, A. Heuer, G. Hinze, S. C. Kuebler, R. Richert, B. Schiener, H. Sillescu, H. W. Spiess, U. Tracht, and M. Wilhelm, "Nature of the non-exponential primary relaxation in structural glass-formers probed by dynamically selective experiments," J. Non-Cryst. Solids **235-237**, 1 (1998).
- (32) R. Richert, "Supercooled liquids and glasses by dielectric relaxation spectroscopy," Adv. Chem. Phys. **156**, 101 (2014).
- (33) F. Alvarez, A. Alegria, and J. Colmenero, "Relationship between the time-domain Kohlrausch-Williams-Watts and frequency-domain Havriliak-Negami relaxation functions," Phys. Rev. B **44**, 7306 (1991).
- (34) C. Burger, Ph.D. Thesis, Universität Marburg, Germany, 1994.
- (35) L. C. E. Struik, "Physical aging in amorphous glassy polymers," Ann. New York Acad. Sci. **279**, 78 (1976).
- (36) R. Richert, P. Lunkenheimer, S. Kastner, and A. Loidl, "On the Derivation of Equilibrium Relaxation Times from Aging Experiments," J. Phys. Chem. B **117**, 12689 (2013).
- (37) K. Moch, P. Münzner, C. Gainaru, and R. Böhmer, "Nongeneric structural-relaxation shape of supercooled liquids: Insights from linear and nonlinear experiments on propylene glycol," J. Chem. Phys. **157**, 231101 (2022).

